

1  
2  
3  
4  
5  
6  
7  
8  
9  
10  
11  
12  
13  
14  
15  
16  
17  
18  
19  
20  
21  
22  
23  
24  
25  
26  
27  
28  
29  
30  
31  
32  
33  
34  
35  
36  
37  
38  
39  
40  
41

## Supplementary Information

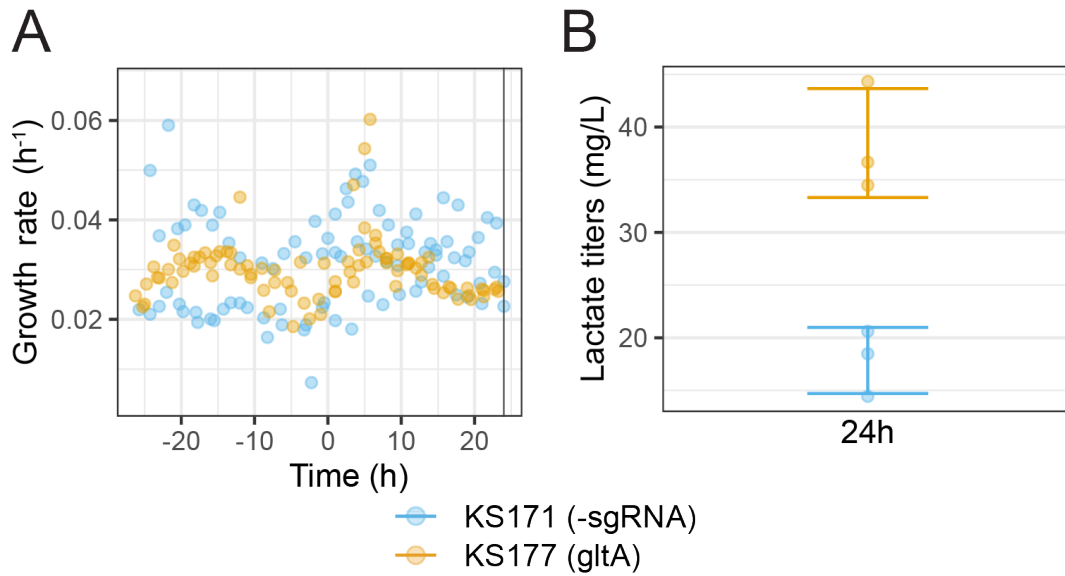
### Cycling between growth and production phases increases cyanobacteria bioproduction of lactate

Kiyan Shabestary, Hugo Pineda Hernandez, Rui Miao, Emil Ljungqvist, Olivia Hallman, Emil Sporre, Filipe Branco dos Santos, Elton P. Hudson

#### Table of contents:

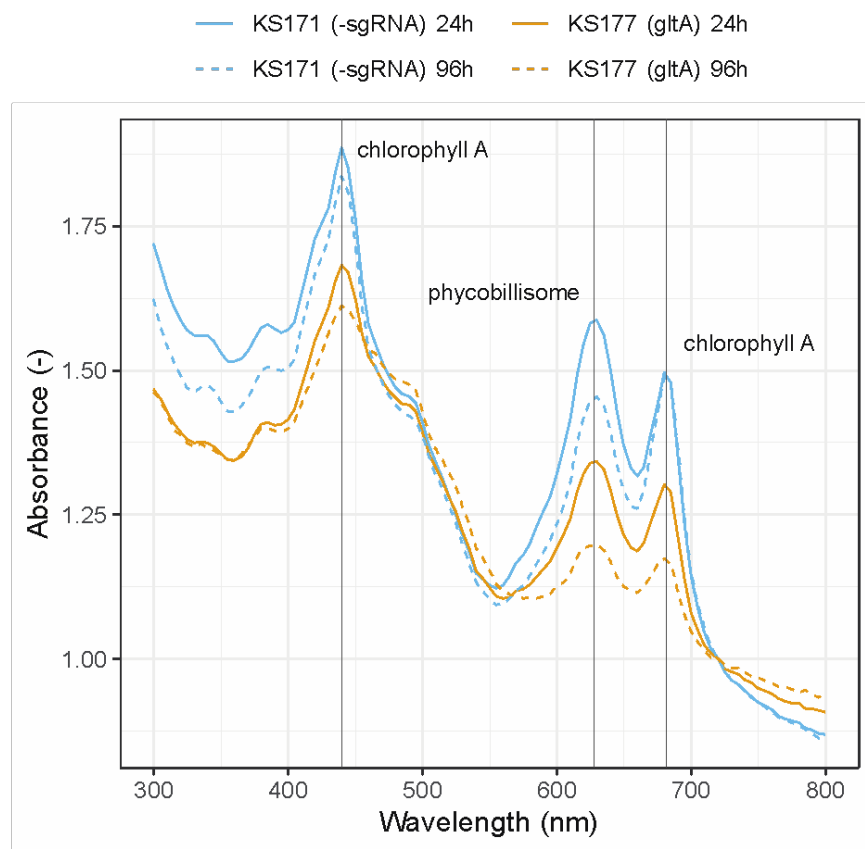
- Figure S1.** Lactate production in a turbidostat setting after 24h.
- Figure S2.** Absorbance spectrum of GA and non-GA KS177 in a batch cultivations.
- Figure S3.** Growth curves for KS177 during growth-arrest with addition of glutamate and aspartate.
- Figure S4.** Chlorophyll A content for GA KS177 supplemented with glutamate and aspartate.
- Figure S5.** Growth curves for KS201 during growth arrest with addition of arginine and alpha-ketoglutarate.
- Figure S6.** Recovery of growth by growth-arrested cells after removal of aTc .
- Figure S7.** Correlation analysis between growth-arrest and published nitrogen starved transcriptome responses.
- Figure S8.** Volcano plot of ribosomal genes for KS177 after 24h and 96h induction.
- Figure S9.** Glycogen accumulation in growth arrested KS177
- Figure S10.** Comparing growth arrest and NADPH accumulation during growth arrest for cells producing lactate and cells not producing lactate.
- Figure S11.** Effect of expressing the cytochrome P450 CYP1A1 on time to reach growth-arrest and CO<sub>2</sub> fixation.
- Figure S12.** Chlorophyll A and lactate production of cultures for the intermittent growth experiment.
- Table S1.** GO term association of the RNAseq response of significantly up-regulated genes after 24h ( $P_{adj} < 0.005$ ).
- Table S2.** List of strains used in this study.
- Supplementary Note 1.** Protocol for proteome analysis.
- Supplementary Note 2.** Calculation of turbidostat production parameters.

42  
43  
44  
45



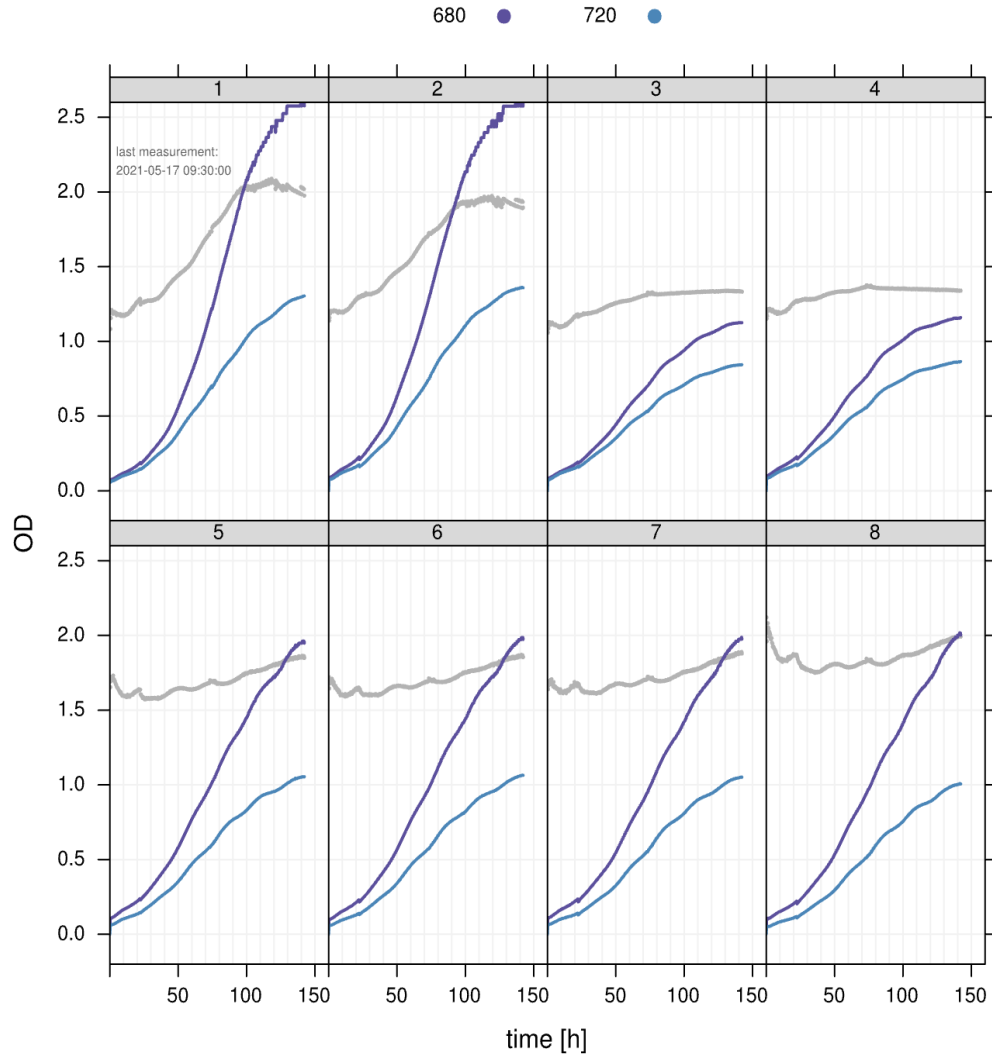
46  
47  
48  
49  
50  
51  
52

**Figure S1.** Growth arrest increases lactate titers compared to non-growth arrested strain. Growth rate and lactate titers for KS171 and KS177 grown in triplicates in turbidostat mode. (A) Growth rate. Addition of aTc to induce CRISPRi was at 0 h. Culture supernatant was sampled 24 h post induction (black line) for lactate titer. (B) Corresponding lactate titers after 24h. The cell density was OD = 0.4 with white light at 200  $\mu$ E.



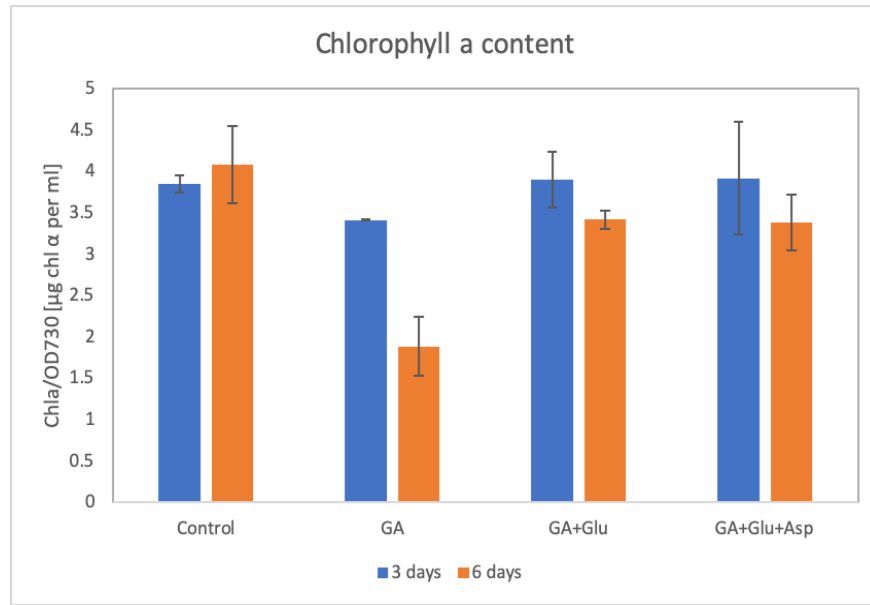
53  
 54 **Figure S2.** Absorbance spectrum for KS171 (no sgRNA) and KS177 (sgRNA targeting *gltA*) at 24 h  
 55 and 96 h post-induction of CRISPRi. Absorbance peaks for chlorophyll A and the  
 56 phycobilisomes are indicated. Cells were grown in a multicultivator in batch mode with a light  
 57 intensity of 300  $\mu$ E. The induction of CRISPRi with aTc was at the start of the experiment when  
 58  $OD_{730} = 0.1$ .

59



60  
61 **Figure S3.** Growth curves for strain KS177 during growth arrest, with added external glutamate  
62 and aspartate to some cultures. Cultures 1-2 are KS177 without aTc (non-arrest control).  
63 Channels 3-4 are KS177 with aTc (growth arrested). Channels 5-6 are KS177 with added aTc and  
64 added 5 mM L-glutamate (pH-adjusted). Channels 7-8 are KS177 with added aTc and 5 mM  
65 glutamate and 5 mM aspartate (pH-adjusted). Addition of glutamate with or without aspartate  
66 could mitigate the growth arrest but not fully. All cultivations were done in batch mode in an MC-  
67 1000 multicultivator. Starting  $OD_{730} = 0.05$ , temperature was 30°C, 1% CO<sub>2</sub> was bubbled into the  
68 cultures, and white light was constant at 150  $\mu\text{mol photons/m}^2/\text{s}$ . Purple lines: recorded  $OD_{680}$ .  
69 Blue lines: recorded  $OD_{720}$ . Gray lines:  $OD_{680}/OD_{720}$ , a measure of pigment content per cell.

70



71

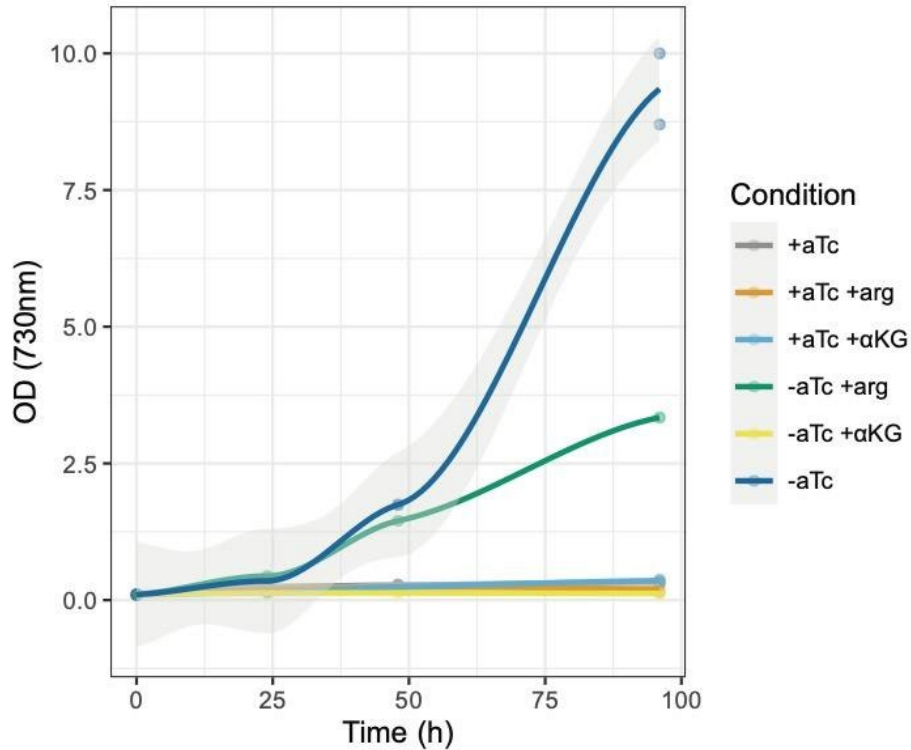
72 **Figure S4.** Chlorophyll A content for strain KS177 during normal growth, during growth-arrest  
 73 with CRISPRi (GA), and during growth arrest with added L-glutamate and L-aspartate (5 mM each,  
 74 pH-adjusted). Addition of L-glutamate to growth-arrested cells increases chlorophyll A levels.  
 75 Starting OD<sub>720</sub> was 0.05 and cells were grown in a Multicultivator at 30°C with 1% CO<sub>2</sub> atmosphere  
 76 and light at 150 µmol photons/m<sup>2</sup>/s.

77

78

79

80



81  
 82 **Figure S5.** Growth curves for strain KS201 (containing the *ktgP* transporter from *E. coli*) during  
 83 normal growth or during growth arrest with added external metabolites 2-oxoglutarate (alph-  
 84 ketoglutarate; αKG) at 1 mM or L-arginine at 1 mM (added at t=0 h). Addition of αKG to 1 mM  
 85 was lethal to cells, and addition of L-arginine to 1 mM was detrimental to growth even without  
 86 induction of CRISPRi (-aTc samples). Strains where CRISPRi was induced had aTc (+aTc) had aTc  
 87 added to 1 μg/mL 1 day prior to t=0 h. Starting OD<sub>730</sub> was 0.1 and cells were grown in an  
 88 incubator at 30°C with 1% CO<sub>2</sub> atmosphere and constant white light with estimated intensity of  
 89 40-80 μmol photons/m<sup>2</sup>/s.

90

91

92

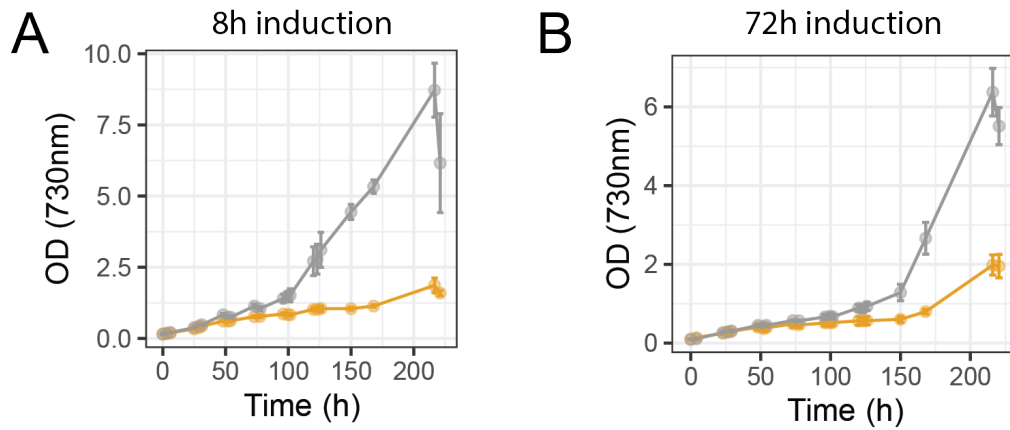
93

94

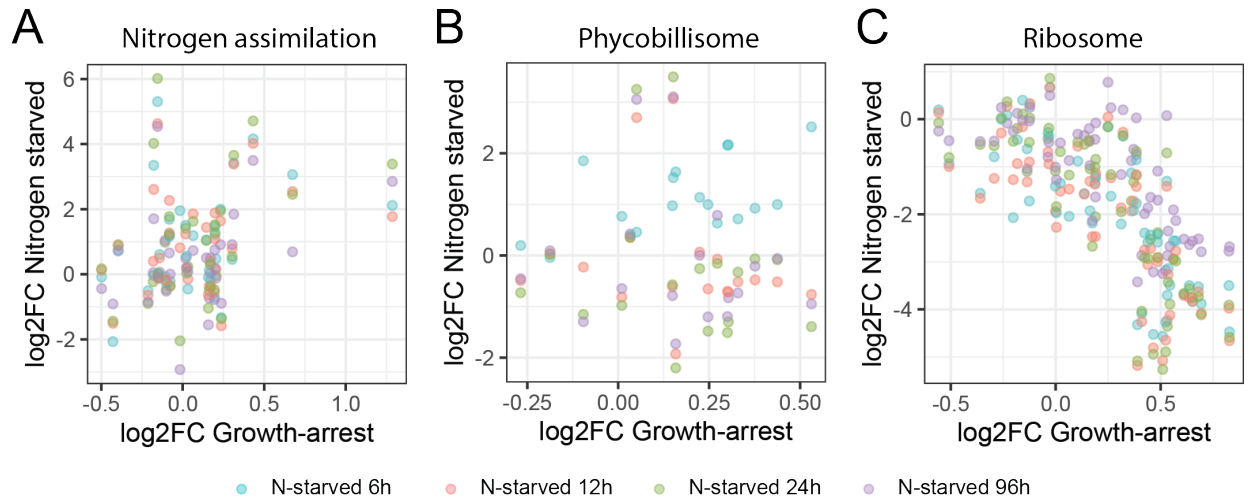
95

96

97



98  
 99 **Figure S6.** Effect of inducer removal on growth-arrested KS177 strain. A seed culture of induced  
 100 KS177 was growth arrested by addition of aTc in a flask (light intensity was 40-80  $\mu\text{mol}$   
 101 photons/ $\text{m}^2/\text{s}$ ). At selected time points after induction (8 h, 72 h) aliquots were taken out,  
 102 washed in BG-11, and used to seed new cultures at  $\text{OD}_{720} = 0.1$ , without aTc (gray lines) or with  
 103 aTc present (orange lines). Cell growth ( $\text{OD}_{720}$ ) was recorded for the new cultures.



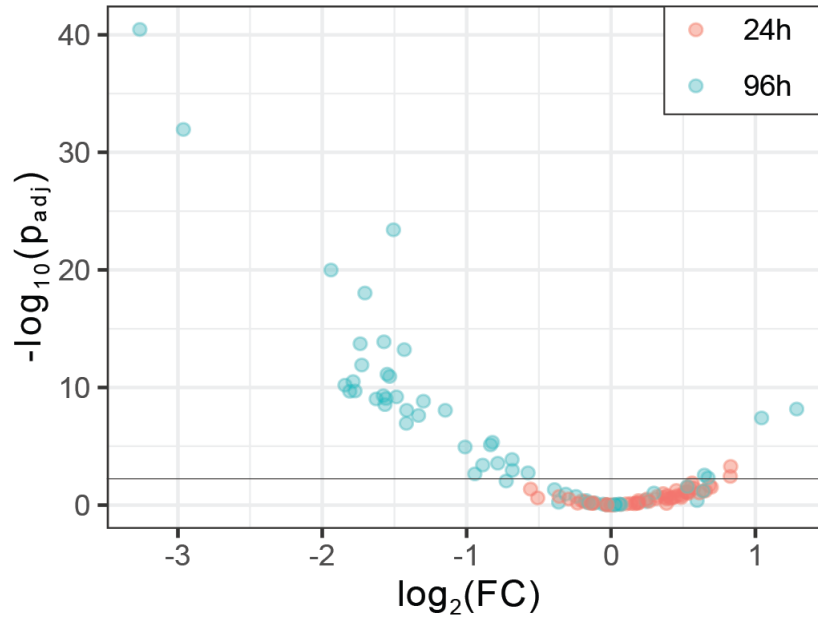
105

106

107 **Figure S7.** Correlation analysis between the *Synechocystis* growth-arrest transcriptome response  
 108 (this work, 24h after induction,  $\text{OD}_{720} = 0.4$ , light =  $200 \mu\text{mol photons/m}^2/\text{s}$ ) and a published  
 109 transcriptome dataset for nitrogen starved *Synechocystis* (Krasikov *et al.*, 2012). Spearman  
 110 correlations were performed for the following subsets: (A) Nitrogen assimilation genes, (B)  
 111 phycobilisome genes and (C) Ribosome genes. Each dot represents one gene. Spearman  
 112 correlations were 0.27, -0.19 and -0.82, respectively. Gene classifications into nitrogen  
 113 assimilation, phycobilisome and ribosome subcategories were obtained from von Wobeser *et al.*  
 114  
 115

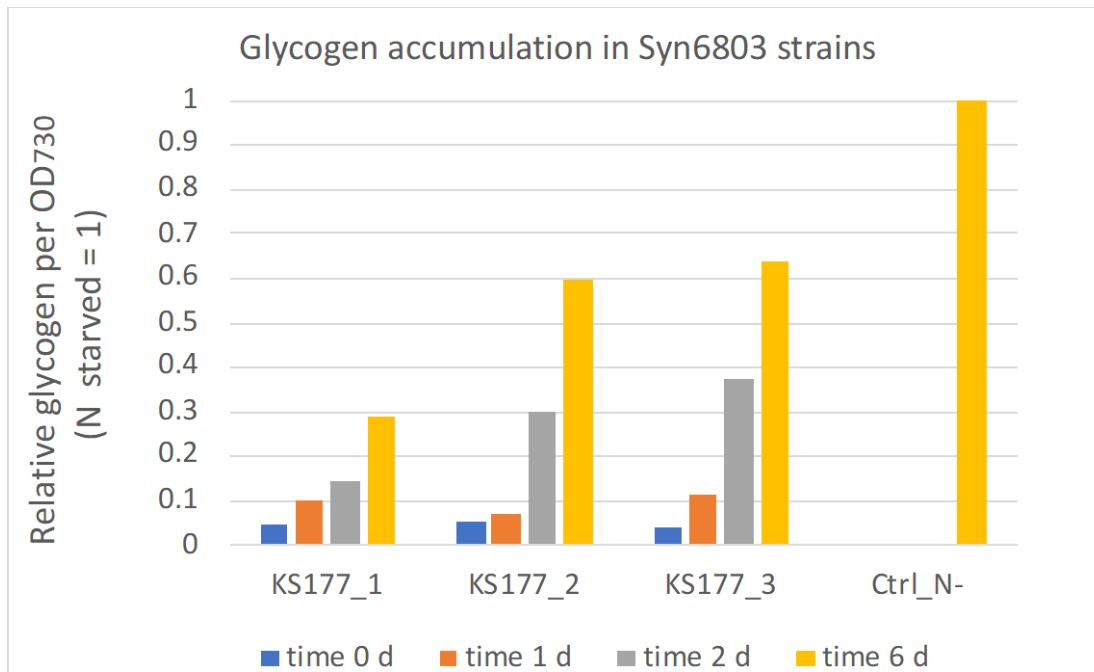


116  
117



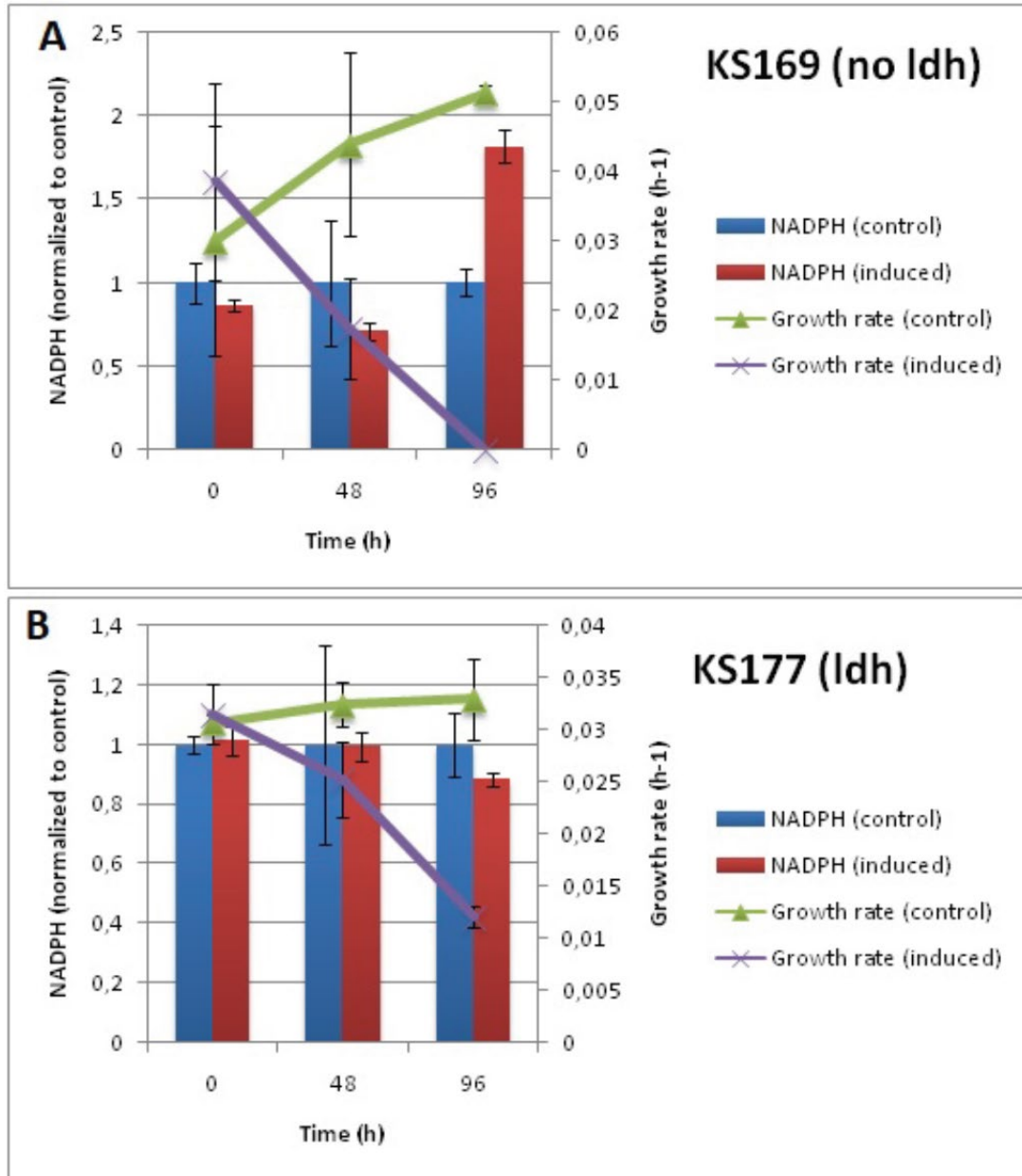
118  
119  
120  
121  
122  
123  
124  
125  
126  
127  
128  
129  
130  
131  
132  
133  
134  
135  
136  
137

**Figure S8.** Volcano plot of the transcriptome response of ribosomal genes for KS177 at 24 h and 96 h post-induction of growth arrest. KS177 was grown in triplicate in turbidostat mode ( $\text{OD}_{720} = 0.4$ , light =  $200 \mu\text{mol photons/m}^2/\text{s}$ ). The horizontal line represents the significance line ( $P_{\text{adj}} = 0.005$ ).

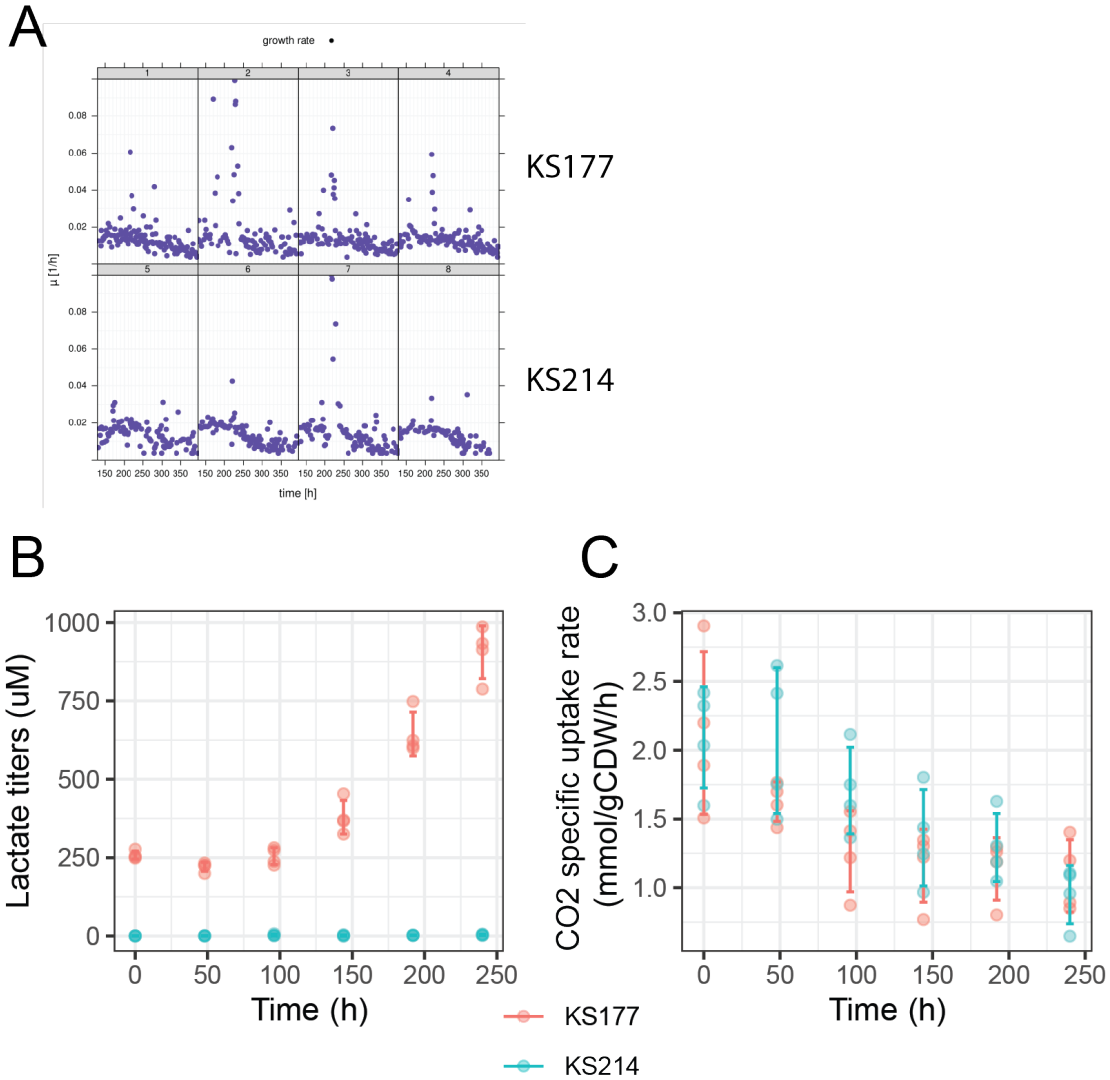


138  
 139  
 140  
 141  
 142  
 143  
 144  
 145  
 146  
 147

**Figure S9.** Glycogen accumulation in KS177 as it enters growth arrest. Three separate cultures of KS177 were started in turibodstat (OD720 =0.2, light = 100 uE). After cultures were stabilized, aTc was added to induce growth arrest (t 0). Samples (15 mL) were taken at 1 d, 2 d, and 6 d post induction for glycogen assay following Koch et al., 2020. By 6 d all KS177 cultures had severely reduced growth rate (50-80% reduction). As a control, a separate KS177 strain (no aTc induction) was washed and resuspended in BG110 media, which has no nitrate. Nitrogen starvation is known to cause glycogen accumulation in *Synechocystis* (Koch et al., 2020). After 6 days, this sample was assayed for glycogen. The relative glycogen content in KS177 cells are reported as normalized of the glycogen content in nitrogen starved cells.

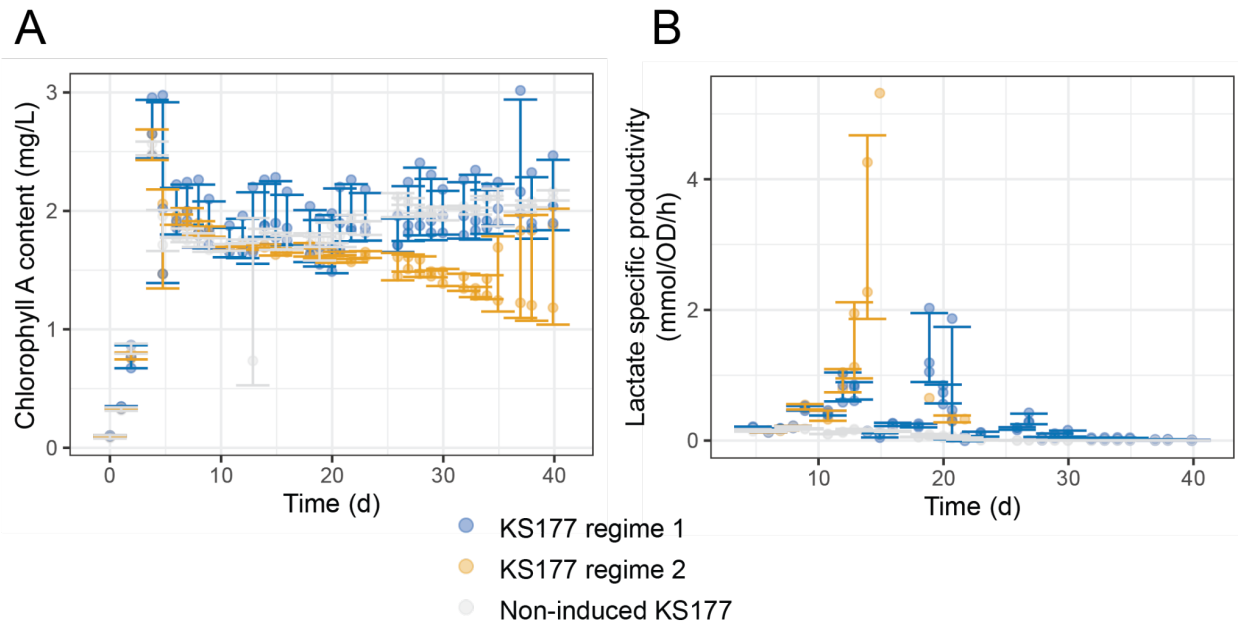


148  
 149 **Figure S10.** A comparison of the effect of the lactate sink (Ldh-catalyzed lactate formation) on  
 150 growth-arrest and resulting NADPH accumulation. KS169 is a strain containing CRISPRi targeting  
 151 *gltA*, but no *Ldh* gene (cannot synthesize lactate). KS177 is a *Synechocystis* strain containing  
 152 CRISPRi and the *Ldh* gene (can synthesize lactate). Strains were grown in turbidostat mode ( $OD_{730}$   
 153 = 0.4, 200  $\mu\text{mol photons/m}^2/\text{s}$ ) in a Multicultivator. At time  $t=0$ , aTc was added to induce growth-  
 154 arrest. Growth rate was recorded and intracellular NADPH was assayed using a fluorescence-  
 155 based assay (Sigma). NADPH levels for each strain are normalized to the uninduced (control)  
 156 culture at each timepoint. The KS169 strain accumulates NADPH during growth-arrest, while the  
 157 lactate-producing KS177 does not. The KS169 strain was completely growth arrested after 96 h,  
 158 while KS177 retained some growth at that time point.  
 159



160  
 161 **Figure S11.** Effect of expression of cytochrome P450 CYP1A1 on growth-arrest in lactate-  
 162 producing *Synechocystis*. (A) Growth rates for KS177 (top panel, no CYP1A1) and KS214 (bottom  
 163 panel, with CYP1A1 from *Mus musculus* expressed). (B) Lactate amount in the turbidostat for  
 164 both strains. (C) Specific CO<sub>2</sub> uptake rates for both strains. Cells were cultivated in a turbidostat  
 165 mode with an OD<sub>720</sub> = 0.4 and a white light intensity of 60 μmol photons/m<sup>2</sup>/s.. KS214 had CYP1A1  
 166 under PpsbA2 promoter inserted at the *slr0397* locus. Active CYP1A1 enzyme in KS214 was  
 167 confirmed using the ethoxyresorufin O-deethylation (EROD) assay as described in Berepiki *et al.*,  
 168 2016 (data not shown).

169  
170



171  
172

173 **Figure S12.** Chlorophyll A and lactate specific productivity for the intermittent growth-arrest  
174 experiments. Chlorophyll A contents were estimated from  $A_{680}$  and  $A_{720}$  absorbance values  
175 (Supplementary Note 2). Cells were cultivated in a turbidostat mode with an  $OD_{720} = 1$  and a light  
176 regime of  $110 \mu\text{mol photons/m}^2/\text{s}$ . Regime 1 was performed in triplicate cultivations. Regime 2  
177 and the control regime were performed in duplicate cultivations. Specific lactate productivity of  
178 each culture was calculated using two sequential lactate concentration measurements and the  
179 dilution rate of the turbidostat.

180  
181  
182

183 **Table S1.** GO term enrichment for genes significantly upregulated ( $P_{adj} < 0.005$ ) at the  
184 transcriptome level in KS177 at 24 h after CRISPRi induction.

GO biological process complete	fold enrichment	raw pvalue	false-discovery rate
response to heat (GO:0009408)	28.59	4.74E-05	4.45E-02
response to temperature stimulus (GO:0009266)	28.59	4.74E-05	2.97E-02
protein folding (GO:0006457)	13.54	1.46E-05	2.74E-02

185

186

187  
188

**Table S2.** List of *Synechocystis* PCC 6803 strains used in this study.

Strain ID	Genotype	Phenotype
KS169	$\Delta$ psbA1::PL22 dCas9 SpR $\Delta$ slr2030–2031::PL22 sgRNA-gltA_33 gltA_155 NatR	Can be growth-arrested by addition of aTc. Not lactate producing
KS171	$\Delta$ psbA1::PL22 dCas9 SpR $\Delta$ slr0168::Ptrc ldh CmR	Cannot be growth-arrested by addition of aTc .Lactate producing.
KS177	$\Delta$ psbA1::PL22 dCas9 SpR $\Delta$ slr0168::Ptrc ldh CmR $\Delta$ slr2030–2031::PL22 sgRNA-gltA_33 gltA_155 NatR	Can be growth-arrested by addition of aTc. Lactate producing
KS201	$\Delta$ psbA1::PL22 dCas9 SpR $\Delta$ slr0168::Ptrc ldh CmR $\Delta$ slr2030–2031::PL22 sgRNA-gltA_33 gltA_155 NatR $\Delta$ slr0397::PpsbA2 kgtP GmR	Can be growth-arrested by addition of aTc. Lactate producing. Constitutive expression of KgtP transporter from <i>E. coli</i> .
KS214	$\Delta$ psbA1::PL22 dCas9 SpR $\Delta$ slr0168::Ptrc ldh CmR $\Delta$ slr2030–2031::PL22 sgRNA-gltA_33 gltA_155 NatR $\Delta$ slr0397::PpsbA2 CYP1A1 GmR	Can be growth-arrested by addition of aTc. Lactate producing. Constitutive expression of cytochrome P450 enzyme CYP1A1 from <i>M. musculus</i> .

189  
190  
191  
192  
193

Sp: spectinomycin; Km: kanamycin, Gm: gentamicin, Cm: chloramphenicol; Nat: nourseothricin

194 **Supplementary Note 1: Protocol for proteome analysis.**

195

196 Lysis and protein quantification

197

198 Frozen samples were brought out of -80 °C storage and thawed on ice. They were then lysed  
199 mechanically through rigorous shaking by a FastPrep-24 5G lysis machine over six cycles of 45  
200 seconds, 6.5 m/s with 30 seconds on ice between cycles. The lysate was centrifuged for 5 min at  
201 21,000g and 4 °C. The resulting supernatant was run through a Zeba Spin Desalting column for 2  
202 min at 1,500g and 4 °C. The protein concentration was then evaluated through a Bradford assay.

203

204 Digestion

205

206 The samples were then incubated at 96 °C for 3 min. Afterwards, sodium deoxycholate and DTT  
207 were added to all samples to final concentrations of 5 % and 10 mM respectively after which the  
208 samples were again incubated at 96 °C for 10 min. Iodoacetamide was added to each sample to  
209 a final concentration of 10 mM for alkylation, followed by 30 min of room temperature  
210 incubation in the dark. Finally, the samples were diluted 10X in ammonium bicarbonate 100 mM  
211 and digested by 0.2 µg/µL LysC at 37 °C, 400 RPM, for 3h followed by digestion by 0.2 µg/µL  
212 Trypsin at 37 °C, 400 RPM, for 16h overnight. Digestion was halted by addition of formic acid to  
213 reduce pH below 2 which caused sodium deoxycholate to precipitate. Samples were then  
214 centrifuged at 14,000g for 10 min after which the supernatant was removed and stored at -20 °C.

215

216 Peptide purification and LC – MS/MS analysis

217

218 Frozen peptide mixes were thawed to room temperature and loaded 325 µL onto activated C18  
219 columns. The columns were then washed with 0.1 % formic acid after which the samples were  
220 eluted with 80 % acetonitrile – 0.1 % formic acid. The resulting peptide mixes were dried in a  
221 vacuum centrifuge and stored in -20 °C for several weeks until the mass spectrometry machine  
222 was available. At that point, the peptides were resuspended in 10 µL 0.1 % formic acid and  
223 analyzed by LC – MS/MS utilizing a Q-exactive HF Hybrid Quadrupole-Orbitrap Mass  
224 Spectrometer coupled with an UltiMate 3000 RSLCnano System with an EASY-Spray ion source.  
225 2 µL of each sample was loaded onto a C18 Acclaim PepMap 100 trap column (75 µm x 2 cm, 3  
226 µm, 100 Å) with a flow rate of 7 µL per min, using 3 % acetonitrile, 0.1 % formic acid and 96.9 %  
227 water as 6 solvent. The samples were then separated on ES802 EASY-Spray PepMap RSLC C18  
228 Column (75 µm x 25 cm, 2 µm, 100Å) with a flow rate of 3.6 µL per minute for 40 minutes using  
229 a linear gradient from 1 to 32 % with 95 % acetonitrile, 0.1 % formic acid and 4.9 % water as  
230 secondary solvent. After separation MS analysis was performed using one full scan (resolution  
231 30,000 at 200 m/z, mass range 300 – 1200 m/z) followed by 30 MS2 DIA scans (resolution 30,000  
232 at 200 m/z, mass range 350 – 1000 m/z) with an isolation window of 10 m/z. Precursor ion  
233 fragmentation was performed with high-energy collision-induced dissociation at an NCE of 26.  
234 The maximum injection times for the MS1 and MS2 were 105 ms and 55 ms respectively, and the  
235 automatic gain control was set to 3e6 and 1e6 respectively. The EncyclopeDIA and Prosit  
236 workflows were used to generate a predicted library from a fasta file of *Synechocystis* proteome  
237 against which an EncyclopeDIA search was performed to generate a list of detected peptides.



238  
239  
240  
241  
242  
243  
244  
245  
246  
247  
248  
249  
250  
251  
252  
253  
254  
255  
256  
257  
258  
259  
260  
261  
262  
263  
264  
265  
266  
267  
268  
269  
270  
271  
272  
273  
274  
275  
276

## Data analysis

The output of the LC – MS/MS analysis was in the form of a list of peptides, their protein of origin and detected intensity. Each timepoint was considered a separate experiment in which the intensity of every detected peptide was compared to the intensity of that same peptide in the first timepoint sample. Peptides not present in all timepoints were excluded from the result. Statistical analysis was performed group-wise with the MSstats package in R. A significant peptide was defined as one that has an absolute log<sub>2</sub>FC of at least 1 and a q-value of less than 0.01, meaning the False Discovery Rate (FDR) was set to 1 %. The data was searched using EncyclopeDIA (Searle *et al.*, 2018) against a predicted library generated with Prosit (Gessulat *et al.*, 2019).

## **Supplementary Note 2.** Calculation of turbidostat production parameters.

The carbon partitioning and cumulative lactate titer in the turbidostat experiment were estimated as follows. First the dilution percentage for each turbidostat cycle was calculated based on the recorded Multi-Cultivator OD<sub>720</sub> before and after pumps were activated. Using the dilution percentage, the theoretical lactate concentration was calculated assuming no lactate was produced after each lactate measurement. The difference between this value and the measured lactate concentration in the consecutive sampling point was taken as the amount of lactate produced. The same approach was followed to estimate the amount of biomass produced between sampling points, based on the external OD<sub>730</sub> measurements.

The cumulative lactate titer was then calculated as the sum of all the differences between theoretical and measured lactate concentrations. The carbon partitioning was calculated as the amount of carbon diverted into lactate divided by the sum of carbon in lactate and biomass. To obtain the amount of carbon in biomass, a conversion factor of 0.148 g / L \* OD<sub>730</sub> was applied and the biomass molecular composition was assumed to be C<sub>4</sub>H<sub>7</sub>O<sub>2</sub>N (Du *et al.*, 2016).

In cases where Chl a content was estimated from cell absorbance spectra, we used an empirical formula,  $10.186 \cdot (OD_{680} - OD_{730}) - 0.08 = \text{mg Chl a L}^{-1}$  (Inskeep and Bloom, 1985).

277   References

278

279   Berepiki, A., Hitchcock, A., Moore, C. M. & Bibby, T. S. Tapping the Unused Potential of  
280   Photosynthesis with a Heterologous Electron Sink. *ACS Synthetic Biology* **5**, 1369–1375 (2016).

281   Du, W. *et al.* Photonfluxostat: A method for light-limited batch cultivation of cyanobacteria at  
282   different, yet constant, growth rates. *Algal Research* **20**, 118–125 (2016).

283   Gessulat, S. *et al.* Prosit: proteome-wide prediction of peptide tandem mass spectra by deep  
284   learning. *Nature Methods* **16**, 509–518 (2019).

285   Inskeep, W. P. & Bloom, P. R. Extinction Coefficients of Chlorophyll a and b in N,N -  
286   Dimethylformamide and 80% Acetone. *Plant Physiology* **77**, 483–485 (1985).

287   Koch M., Doello S., Gutekunst K., Forchhammer K., 2019. PHB is produced from glycogen  
288   turnover during nitrogen starvation in *Synechocystis sp.* PCC 6803. *Intl. J. Mol. Sci.* 20, 1942.  
289   <https://doi.org/10.3390/ijms20081942>.

290

291   Krasikov, V., Aguirre von Wobeser, E., Dekker, H. L., Huisman, J. & Matthijs, H. C. P. Time-series  
292   resolution of gradual nitrogen starvation and its impact on photosynthesis in the cyanobacterium  
293   *Synechocystis* PCC 6803. *Physiologia Plantarum* **145**, 426–439 (2012).

294   Searle, B. C. *et al.* Chromatogram libraries improve peptide detection and quantification by data  
295   independent acquisition mass spectrometry. *Nature Communications* **9**, (2018).

296

297   von Wobeser, E. A. *et al.* Concerted changes in gene expression and cell physiology of the  
298   cyanobacterium *Synechocystis sp.* strain PCC 6803 during transitions between nitrogen and light-  
299   limited growth. *Plant Physiology* **155**, 1445–1457 (2011).

300

301

302